REMEDIATION OF TROPICAL SOIL CONTAMINATED WITH POLYCYCLIC AROMATIC HYDROCARBONS THROUGH ADVANCED OXIDATION PROCESS

MOHAMMAD ISAM MOHAMMAD QUTOB

UNIVERSITI SAINS MALAYSIA

2024

REMEDIATION OF TROPICAL SOIL CONTAMINATED WITH POLYCYCLIC AROMATIC HYDROCARBONS THROUGH ADVANCED OXIDATION PROCESS

by

MOHAMMAD ISAM MOHAMMAD QUTOB

Thesis submitted in fulfilment of the requirements for the degree of Doctor of Philosophy

December 2024

ACKNOWLEDGEMENT

I would first like to give reverence to Allah Almighty, who made all things possible. Then, I would like to thank my parents for their emotional and financial support during my PhD journey.

I want to express my gratitude to Assoc. Prof. Dr. Mohd Rafatullah, who walked with me step by step on the path of scientific research until we were able to publish in prestigious scientific journals. He was also my main supervisor for more than three years, during which I learned multiple skills from him.

It is my pleasure to thank my previous co-supervisor and now main supervisor, Dr. Syahidah Akmal Binti Muhammad, for her support in the lab practice, drafting my thesis, and providing advice.

I highly appreciate the assistance of Prof. Dr. Norli Ismail and Assoc. Prof. Dr. Japareng Lalung for granting permission to use their lab tools and equipment during my experiments.

I am very thankful to my friends whose fellowship helped me in both my personal life and academic success. Special mention goes to Fozy Binhweel, Dani Wijaya, and Hamza Mohamed Flafel.

May Allah bless us all!

Mohammad Qutob

December 2024

TABLE OF CONTENTS

LIST OF TABLES

Page

LIST OF FIGURES

LIST OF SYMBOLS

Σ	Summation symbol, indicating a total or sum
λ	Lambda, the unit of wavelength
λ_{max}	Maximum lambda
$\leq$	Less than or Equal
$<$	Less than
%	Percent
°	Degree
′	Minute
″	Second
℃	Degrees Celsius, a unit of temperature
μg/L	Microgram per liter
μg/kg	Microgram per kilogram
μm	Micrometer
μS/m	Microsiemens per meter
$(O_2:N_2)$	Oxygen to nitrogen ratio
δ-MnO_2	Delta-manganese dioxide
[Σ azo dyes]	Summation of azo dyes, indicating a total concentration
[Biochar]	Concentration of biochar
[BTEX]	Concentration of benzene, toluene, ethylbenzene, and xylene
$[Cu(II)]_0$	Initial concentration of Copper(II) ions
[Catalyst]	Concentration of the catalyst
[CPC]	Concentration of cetylpyridinium chloride

[EDTA]	Concentration of ethylenediaminetetraacetic acid
$[Fe^{2+}]$	Concentration of ferrous ions
$[Fe^{3+}]$	Concentration of ferric ions
$[FeCO_3]$	Concentration of iron carbonate
$[H_2O_2]$	Concentration of hydrogen peroxide
[MW power]	Microwave power
$[Na_2SO_4]$	Concentration of sodium sulfate
$[NaNO_3]$	Concentration of sodium nitrate
[Ozone]	Concentration of ozone
[PMS]	Concentration of peroxymonosulfate
$[Pollutant]_0$	Initial concentration of a pollutant
[PS]	Concentration of persulfate
[Surfactant]	Concentration of surfactant
[ZVI]	Concentration of zero-valent iron
€/ton	Euros per metric ton
$^1O_2$	Singlet oxygen
A/m^2	Ampere per square meter
Al 2p	The binding energy of electrons associated with aluminum in the 2p energy level
As	Arsenic
Biochar-MoS_2–Ag	Composite material containing biochar, molybdenum disulfide, and silver

C1s	The binding energy of electrons associated with carbon in the 1s energy level.
(C10-C28)	A range of carbon chain lengths, typically referring to hydrocarbons
(C28-C40)	
(C6-C22)	
(C7 – C23)	
C_3N_4	Cyanamide
C3 and C4	Different pathways in plants for fixing carbon dioxide during photosynthesis.
C_3N_4	Cyanamide
Cr (VI)	Chromium in its hexavalent oxidation state
Ca^{2+}	Calcium ion
Cd	Cadmium
Cl^-	Chloride ion
$cmol_C/kg$	Centimole of cations per kilogram
cm	Centimeter
cm^{-1}	The absorbance unit of FTIR
CMC-Fe_3O_4	Carboxymethyl cellulose-coated iron(II,III) oxide, a composite material
CMC-nZVI/BC	Carboxymethyl cellulose-coated nanoscale zero-valent iron/biochar composite material
$CO3^{\bullet -}$	Carbonate radical
Cr	Chromium

Cu	Copper
Cu (II) or Cu^{2+}	Copper ion, a positively charged ion of copper in its 2+ oxidation state
e^-	Electron
e_{aq}^-	Hydrated electron
Ea	Activation energy
Fe^{2+}	Ferrous ion
Fe 2p	The binding energy of electrons associated with iron in the 2p energy level
Fe_2O_3	Iron oxide
Fe_3O_4@C	Iron oxide embedded in carbon, a composite material.
FeCo	Iron-cobalt alloy
g	Gram
g/L	Gram per liter
g/cm^3	Gram per cubic centimeter
g/kg	Grams per kilogram
GO_x	Graphene oxide
$H^\bullet$	Hydrogen radical
$H_2O_2:Fe^{2+}$	Ratio of hydrogen peroxide to ferrous ions
$HO^\bullet$	Hydroxyl radicals
$HO_2^\bullet$	Hydroperoxyl radical
hv	Irradiation
k	kinetic reaction rate

K	Kilo
K^+	Potassium ion
K_2SO_4	Potassium sulfate
kGy	Kilogray, a unit of absorbed dose of ionizing radiation
kHz	Kilohertz, which is a unit of frequency
KH_2PO_4	Potassium dihydrogen phosphate
kW	Kilowatt
kWh/ ton	Kilowatt-hour per ton
kW/kg	Kilowatt per kilogram
L/min	Liters per minute, a unit of flow rate
Lux	Unit of illuminance
M	Molarity, a unit of concentration
m^3/hour	Cubic meters per hour
MeV	Million electron volts
mg/L	Milligrams per liter
mg/g	Milligrams per gram, a unit of mass concentration
mg/kg	Milligrams per kilogram
Mg^{2+}	Magnesium ion
$MgFe_2O_4$	Magnesium ferrite
mL/min	Milliliters per minute, a unit of flow rate
mM	Millimolar, a unit of concentration
mmol/g	Millimoles per gram, a unit of concentration
mmol/kg	Millimoles per kilogram, a unit of concentration

mmol/L	Millimoles per liter, a unit of concentration
mol/L	Molar, a unit of concentration
Mn^{2+}	Manganese (II) ion
NaCl	Sodium chloride
ng/g	Nanogram per kilogram
ng/m^3	Nanogram per cubic meter
NH_4NO_3	Ammonium nitrate
Ni	Nickel
Ni^{2+}	Nickel (II) ion
nm	Nanometer
NO_3^-	Nitrate ion
$O^{\bullet -}$	Superoxide radicals
O 1s	The binding energy of electrons associated with oxygen in the 1s energy level
Pb	Lead
pH	A measure of the acidity or alkalinity of a solution
phdCI	Is a functional gene in *Sphingomonas* sp. responsible on the metabolize of PHE
PheN7	Is a functional gene in anaerobic *Bacillus firmus* sp. responsible on the metabolize of PAHs
ppm	Parts per million, a unit of concentration
R	Universal gas constant
RuO_2	Ruthenium oxide

Si 2p	The binding energy of electrons associated with silicon in the 2p energy level
SO_4^{2-}	Sulfate ion
$SO_5^{\bullet-}$	Peroxymonosulfate radical
TiO_2	Titanium oxide
Urea H_2O_2	Mixture of urea and hydrogen peroxide
V	Volt
V/cm	Volts per centimeter
v/v	Volume per volume, a ratio of volumes
W	Watt, a unit of power
W/cm^2	Watts per square centimeter, a unit of power density
wt%	Weight percent
Zn	Zinc

LIST OF ABBREVIATIONS

1,4-Bq	1,4-Benzoquinone
ABS	Wave absorbance
ANT	Anthracene
AOP	Advanced oxidation process
B[α]P	Benzo[α]pyrene
BaA	Benzo(a)anthracene
BAF	Free fungi system
BAW	Wood-assisted fungal system
BC	Biochar
BSM	Basal salt mediums
BTEX	Benzene, toluene, ethylbenzene, and xylene
CA	Ca-alginate
COD	Chemical oxygen demand
CPC	Cetylpyridinium chloride
CEC	Cation exchange capacity
DDBD	Double dielectric barrier discharge
DDT	Dichlorodiphenyltrichloroethane
DNA	Deoxyribonucleic acid
E-E	Edge to Edge
EC_{50}	Half maximal effective concentration
EDX	Dispersive X-ray Spectroscopy
EK	Electrokinetic

EK-F	Electro-Fenton
EO	Electro-osmosis
EPHs	Extractable petroleum hydrocarbons
EPR	Electron Paramagnetic Resonance
F-F	Face to Face
F-E	Face to Edge
FE	Freeze-thaw combined electro-osmosis
FT	Freeze-thaw
FTIR	Fourier Transform Infrared Spectroscopy
FWHM	Full-width at half-maximum
GC-MS	Gas chromatography–mass spectrometry
GHS	Global harmonized system
H	Hematite
HA	Humic acid
HACA	Hydrogen abstraction and acetylene/carbon addition
HAVA	Vinyl acetylene addition
HMW	High molecular weight
HPLC	High-performance liquid chromatography
IARC	International agency for research on cancer
K	Kaolinite
LC_{50}	Lethal concentration 50%
MAC	Methyl addition cyclization
MPE	Multiphase extraction

N/A	Data unavailable
NAP	Naphthalene
nZVI	Nano zero-valent iron
PAHs	Polycyclic aromatic hydrocarbons
PBDEs	Polybrominated diphenyl ethers
PCL	Polycaprolactone
PDS	Peroxydisulfate
PHE	Phenanthrene
PMS	Peroxymonoperdulfate
PS	Persulfate
PSB	Phosphate solubilizing bacteria
PYR	Pyrene
Q	Quartz
qPCR	Quantitative polymerase chain reaction
QSAR	Quantitative Structure-Activity Relationship
rDNA	Ribosomal DNA
RHDa	Ring hydroxylating dioxygenases
ROS	Reactive oxygen species
SC	Sodium citrate
SDBS	Sodium Dodecyl Benzensulphonate
SDGs	Sustainable development goals
SDS	Sodium dodecylsulfate
SEM	Scanning Electron Microscopy

SGE	Nano-sulfonated graphene
SMF	Superoleophilic sponges
SOM	Soil organic matter
TBA	tert-butanol
TEST	Toxicity Estimation Software Tool
Temp	Temperature
TPHs	Total petroleum hydrocarbons
USEPA	United States Environmental Protection agency
UV	Ultraviolet light
XPS	X-ray photoelectron spectroscopy
XRD	X-ray Diffraction

LIST OF APPENDICES

PEMULIHAN TANAH TROPIKA YANG TERCEMAR DENGAN HIDROKARBON AROMATIK POLISIKLIK MELALUI PROSES PENGOKSIDAAN TERMAJU

ABSTRAK

Hidrokarbon aromatik polisiklik (PAH) adalah bahan kimia yang diklasifikasikan sebagai pencemar utama. Sembilan puluh peratus daripada PAH yang dilepaskan ke alam sekitar akhirnya terkumpul di dalam tanah, menjadikan teknik pemulihan tanah yang sesuai amat diperlukan. Proses pengoksidaan termaju (AOP) adalah salah satu kaedah yang paling cekap untuk pemulihan PAH di dalam tanah. Dalam sistem AOP, pemangkin yang berasal dari mineral besi semulajadi menawarkan beberapa kelebihan. Walaubagaimanapun, penggunaannya dalam pemulihan tanah adalah terhad kerana kehadiran kotoran tanah yang boleh menghalang aktiviti pemangkinan mineral ini. Tanah-tanah di kawasan tropika, secara relatifnya, menunjukkan kandungan kotoran tanah yang lebih rendah, justeru meningkatkan kecekapan penggunaan mineral besi semulajadi dari tanah tropika sebagai pemangkin. Dalam hal ini, potensi pemangkinan tanah tropika yang semulajadi berisi besi telah disiasat untuk menghapuskan fenantrena (PHE), pirena (PYR), dan benzo[α]pirena (B[α]P) menggunakan reaktor yang beroksigen yang disokong dengan persulfat (PS). Sistem tersebut menunjukkan prestasi yang cekap, dan kecekapan penyingkiran dengan keadaan optimum adalah masing-masing 81%, 73%, dan 86% untuk PHE, PYR, dan B[α]P. Ini menunjukkan bahawa aktiviti pemangkinan besi berfungsi dengan cekap. Walau bagaimanapun, terdapat perubahan dalam ciri-ciri tanah selepas proses pemulihan seperti pengurangan yang ketara dalam kandungan besi dan aluminium.

Eksperimen hapus-sisa menunjukkan bahawa $HO^{\bullet}$ mempunyai peranan kecil dalam proses pengoksidaan. $SO_4^{\bullet -}$ dan $O_2^{\bullet -}$ muncul sebagai spesies reaktif primer yang bertanggungjawab untuk degradasi PAH yang berkesan. Selain itu, produk sampingan dipantau selepas penambahbaikan tanah untuk menilai ketoksikan mereka dan untuk mencadangkan laluan degradasi. Ujian ketoksikan mendedahkan bahawa beberapa produk sampingan PAH boleh menjadi lebih toksik daripada pencemar induk itu sendiri. Kajian ini mewakili kemajuan yang ketara dalam pemulihan tanah dengan memberikan langkah ke hadapan dalam penggunaan AOP tanpa memerlukan pemangkin tambahan untuk mengaktifkan bahan pengoksida dan menguraikan bahan pencemar PAH dari tanah.

REMEDIATION OF TROPICAL SOIL CONTAMINATED WITH POLYCYCLIC AROMATIC HYDROCARBONS THROUGH ADVANCED OXIDATION PROCESS

ABSTRACT

Polycyclic aromatic hydrocarbons (PAHs) are chemicals classified as priority pollutants. Ninety percent of those released into the environment end up in the soil, which makes suitable soil remediation techniques necessary. Advanced oxidation process (AOP) is one of the most efficient methods for the remediation of PAHs from soil. In AOP systems, the catalysts derived from natural iron minerals offer several advantages. However, their utilization in soil remediation is restricted due to the presence of soil impurities, which can inhibit the catalytic activity of these minerals. The soils in tropical regions relatively low in impurities, this enhances the efficiency of utilizing natural iron minerals from tropical soil as a catalyst. In this regard, the catalytic potential of naturally iron-bearing tropical soil was investigated to eliminate phenanthrene (PHE), pyrene (PYR), and benzo[α]pyrene (B[α]P) using an oxygenated reactor supported with persulfate (PS). The system showed an efficient performance, and the removal efficiencies under the optimum conditions were 81%, 73%, and 86% for PHE, PYR, and B[α]P, respectively. This indicated that the catalytic activity of iron was working efficiently. However, there were changes in the soil characteristics after the remediation process such as a significant reduction in iron and aluminum contents. The scavenging experiments demonstrated that $HO^{\bullet}$ had a minor role in the oxidation process. $SO_4^{\bullet-}$ and $O_2^{\bullet-}$ emerged as the primary reactive species responsible for the effective degradation of the PAHs.

Moreover, the by-products were monitored after soil remediation to evaluate their toxicity and to propose degradation pathways. The toxicity tests revealed that certain PAHs by-products could be more toxic from the parent pollutant itself. This study represents a notable progression in soil remediation by providing a step forward in the application of the AOP without requiring additional catalysts to activate oxidants and degrade pollutant PAHs from the soil.

CHAPTER 1

INTRODUCTION

1.1 Research background

PAHs are compounds that contain two or more benzene rings. PAHs became a reason for concern due to their special properties, which included semi-volatility, lengthy half-lives, resistive nature, negative toxicological impact, long-range transport before deposition, transformation, high lipophilicity, low water solubility, halogenated, and bioaccumulation ability (Adebusuyi et al., 2022; El-Shahawi et al., 2010; Hussain et al., 2018). According to the transboundary property of PAHs, they have been detected in many sensitive places like groundwater and polar regions (Wang et al., 2019). The environmental monitoring of PAHs began more than 40 years ago since 1980s, from that time, the researchers have been concerned about PAHs because of their toxicity and frequent occurrence in the atmosphere, soil, water, and sediment ecosystems (Qiao et al., 2022). Based on that, the United States Environmental Protection Agency (USEPA) listed 16 PAHs as priority pollutants included indeno(1,2,3-cd) pyrene, dibenzo(a,h)anthracene, B[α]P, acenaphthylene, benzo(b)fluoranthene, naphthalene, benzo(k) fluoranthene, chrysene, acenaphthene, benzo(a)anthracene, fluorene, PYR, benzo(g,h,I)perylene, PHE, and fluoranthene (Y. Li et al., 2023).

According to the literature, the PAHs compounds could be released from two major sources (i) natural sources such as forest fires, natural leakage, volcanic eruption, biological sources like diagenesis (organic transformation), and biogenic sources (plant, microbes, algae), and (ii) anthropogenic sources (manmade) such as combustion sources (incomplete combustion of petroleum, gas, wood, etc). In general, the input of PAHs that come from natural sources is less than that from anthropogenic ones. Whatever the PAHs source, their mobility could be done through different pathways such as air deposition, river runoff, home and industrial emissions, direct spills of petroleum, etc (Wolska et al., 2012).

1.2 The Soil remediation techniques based on AOP

It has been reported that 90% of released PAH compounds eventually make their way into the soil matrices (Dai et al., 2022; Sun et al., 2020). Therefore, it is crucial to develop effective soil remediation techniques to prevent their negative impacts on public health and the ecosystem. Many efficient systems have been applied to eliminate PAHs from soils using physical, chemical, and biological agents. AOP systems have been widely used for soil remediation from PAHs (Dai et al., 2022). AOPs considered one of the efficient soil remediation techniques utilized for the elimination of chemicals with high resistance to degradation by the traditional methods (Zhao et al., 2018). The AOP is a chemical procedure dependent on triggering oxidizing agents like PS or hydrogen peroxide through a catalyst, leading to the production of a molecule termed a "radical". These radicals act to attack the organic pollutants and convert them into CO_2, H_2O , and NO_3^- or byproducts (Liu et al., 2023).

The main difference between the oxidation process and AOPs; the oxidation is a fundamental chemical reaction involving electron loss, AOPs are specialized processes that use powerful oxidants to purify water, treat wastewater, and remediate soil by breaking down harmful contaminants.

Researchers have performed numerous studies delving into the theory and application of AOPs, achieving notable advancements. Consequently, novel catalysts have been created to address the limitations of conventional catalysts in the implementation of AOPs (Liu et al., 2021). For instance, electrochemical oxidation, photocatalytic, Sono catalytic, AOP-based micro and nanomaterials catalysts, and AOP-based chemical catalysts (Preethi et al., 2024).

The radicals that attack the target pollutants are varied in their half-life and redox potential, the following are the most frequent radicals that have been generated in AOP systems: sulfate radical ($SO_4^{\bullet -}$, 2.5 ~ 3.1 V), hydroxyl radicals ($HO^{\bullet}$, 2.7 V), peroxymonosulfate radical ($SO_5^{\bullet -}$, 1.1 V), hydrogen radical ($H^{\bullet}$, −2.3 V), hydrated electron (e_{aq}^{-}, −2.9 V), superoxide radicals ($O^{\bullet -}$, 2.4 V), hydroperoxyl radical ($HO_2^{\bullet}$, 1.7 V). and singlet oxygen ($^1O_2$, 2.2 V) (Wang & Wang, 2020).

Among AOP systems, the iron minerals-based catalyst offers several advantages, such as cost-effectiveness, high efficiency, wide availability, and eco-friendliness. Moreover, these minerals have unique structures and properties that ensure stability when exposed to chemical solutions (Liu et al., 2023). Naturally occurring iron minerals, including pyrite, pyrrhotite, mackinawite, goethite, hematite, etc., constitute approximately 7% by weight of the Earth's top crust and are widespread in soils, which have gathered growing interest (Peys et al., 2022).

1.3 Problem statements and research objectives

The large-scale application of AOP using iron-based catalysts for in-situ soil remediation can significantly increase the overall cost. At the same time, approximately 7% of the Earth's top crust contains iron minerals, which are abundant in soils. However, the catalytic activity of these natural iron minerals can be hindered by soil impurities such as anions, cations, and soil organic matter (SOM) (H. Liu et al., 2023). These impurities restrict the effective use of naturally occurring iron in soil as a catalyst to activate oxidants.

Tropical soils, however, are relatively low in such impurities (Bruijnzeel, 1991). The high temperatures and heavy rainfall in tropical regions lead to rapid weathering of rocks and minerals, reducing the presence of impurities (Crasweu & Lefroy, 2001; Fujii, 2014). Additionally, some tropical soils contain high levels of iron oxides (Colombo et al., 2014), which could improve the efficiency of using natural iron minerals as catalysts.

Therefore, this study investigated the catalytic activity of iron content that naturally occurs in tropical soil for activating oxidants and removing PAHs. Despite the potential of AOP, it requires additional chemicals for complete mineralization, which may alter soil characteristics and leave toxic by-products. Nevertheless, the literature addressing these issues remains limited, highlighting a significant knowledge gap.

In this regard, the specific objectives of this study are as follows:

1. To characterize the soil before and after the remediation process
2. To investigate the removal efficiency and mineralization of PHE, PYR, and B[α]P by AOP system based on the natural iron content as a catalyst under different experimental conditions.

3. To propose the activation and removal mechanisms of the PAHs from the soil.
4. To monitor the by-products, build degradation pathways, and evaluate their toxicity.

This research represents a significant advancement in soil remediation by demonstrating the application of the AOP system without the need for additional catalysts to activate oxidants and degrade PAHs in soil. This approach promotes sustainability by reducing the reliance on extra materials, offering a cost-effective and environmentally friendly method for degrading PAHs in contaminated soil.

CHAPTER 2

LITERATURE REVIEW

2.1 PAHs background

Natural events like forest fires and volcanic eruptions can cause the release of PAHs since they are created when incomplete combustion of organic materials occurs (Liao & Yu, 2020; Okedere & Elehinafe, 2022). However, anthropogenic activities including burning biomass, making coke, using thermal industrial processes, driving, and burning rubbish considered the most PAHs emissions (Howsam & Jones, 1998). According to the International Agency for Research on Cancer (IARC), B[α]P is one of the priority PAHs that is most likely to cause cancer. B[α]P is chosen as a marker for PAH pollution, according to world health organization the concentration of B[α]P should not excessed 0.7 µg/l in drinking water, and for other PAHs typical concentration range for a sum of selected PAHs in drinking water is from about 1 to 11 µg/L (WHO, 2017).

2.1.1 PAHs formation mechanisms

It has been reported that most of the PAH's compounds that are released into the environment come from the incomplete combustion process either from a natural event or anthropogenic activity. The researchers proposed different mechanisms for the formation of PAHs, and we can summarize them into three main mechanisms (i) the formation of PAHs via the addition of acetylene or hydrogen abstraction, (ii) the formation of PAHs via vinyl acetylene additions, and (iii) the formation of PAHs via adding radicals.

2.1.1(a) The formation of PAHs by addition of acetylene (C_2H_2)

The formation of PAHs via the addition of acetylene or hydrogen abstraction and acetylene/carbon addition (HACA) could describe the formation of PAHs either if the source was anthropogenic activity or natural events. HACA is the most common reaction mechanism for the formation of PAHs and has attracted growing attention over the past few decades as one of the key PAH formation pathways. Basically, in the addition step of acetylene to the PAHs radical, the low reaction reversibility and the high affinity of hydrogen atoms cause the PAHs to build up continually. In addition, the reaction steps of the HACA also exhibit substantial exothermicity and comparatively low reaction barriers. These facts make it possible to readily overcome the energy barriers that arise during HACA reactions (Reizer et al., 2022). The presence of reactants in different forms (butadiene, butane, benzene, toluene, methane, ethane, ethylene, dimethyl ether, phenylacetylene, heptane, etc.) acting to increases the probability of the formation of PAHs (**Figure 2.1A**).

2.1.1(b) The formation of PAHs by the addition of vinyl acetylene

The formation of PAHs via vinyl acetylene additions (HAVA) was proposed for the first time by (Reizer et al., 2022). Because there is a lot of vinyl acetylene in the combustion environment of different types of flame, which increases the opportunity for HAVA to happen. It has been reported that the formation of a benzene ring is easy in the presence of vinyl acetylene and carbon species. Because of the double and triple bonds in vinyl acetylene, its carbon atoms are extremely active and are used to attack the C atoms in PAHs. The occurrence of PAHs via the HAVA mechanism can be described with two major steps illustrated in **Figure 2.1(B)**, after a PAH radical is created, the HAVA mechanism allows for the formation of a new ring by (i) adding vinyl acetylene to the radical and then (ii) cyclizing it.

2.1.1(c) The formation of PAHs by radicals

Radicals among the various chemical species have a special function in the development of PAHs. Different reaction processes are feasible by utilizing less or more stable carbon-centered radicals, depending on the type of radicals. Several PAHs formation based on radicals have been proposed Such as (i) methyl addition cyclization (MAC), (ii) ethynyl radical, (iii) phenyl addition cyclization, and (iv) resonantly stabilized radicals. To describe the mechanism, we choose methyl radical as one of the most basic but also prevalent alkyl radicals. As illustrated in **Figure 2.1(C)**, In the MAC mechanism, two or three methyl radicals are added to the appropriate PAHs to form an ethyl or propyl chain, followed by hydrogen eliminations and cyclization to produce new aromatic rings (Reizer et al., 2022)**.**

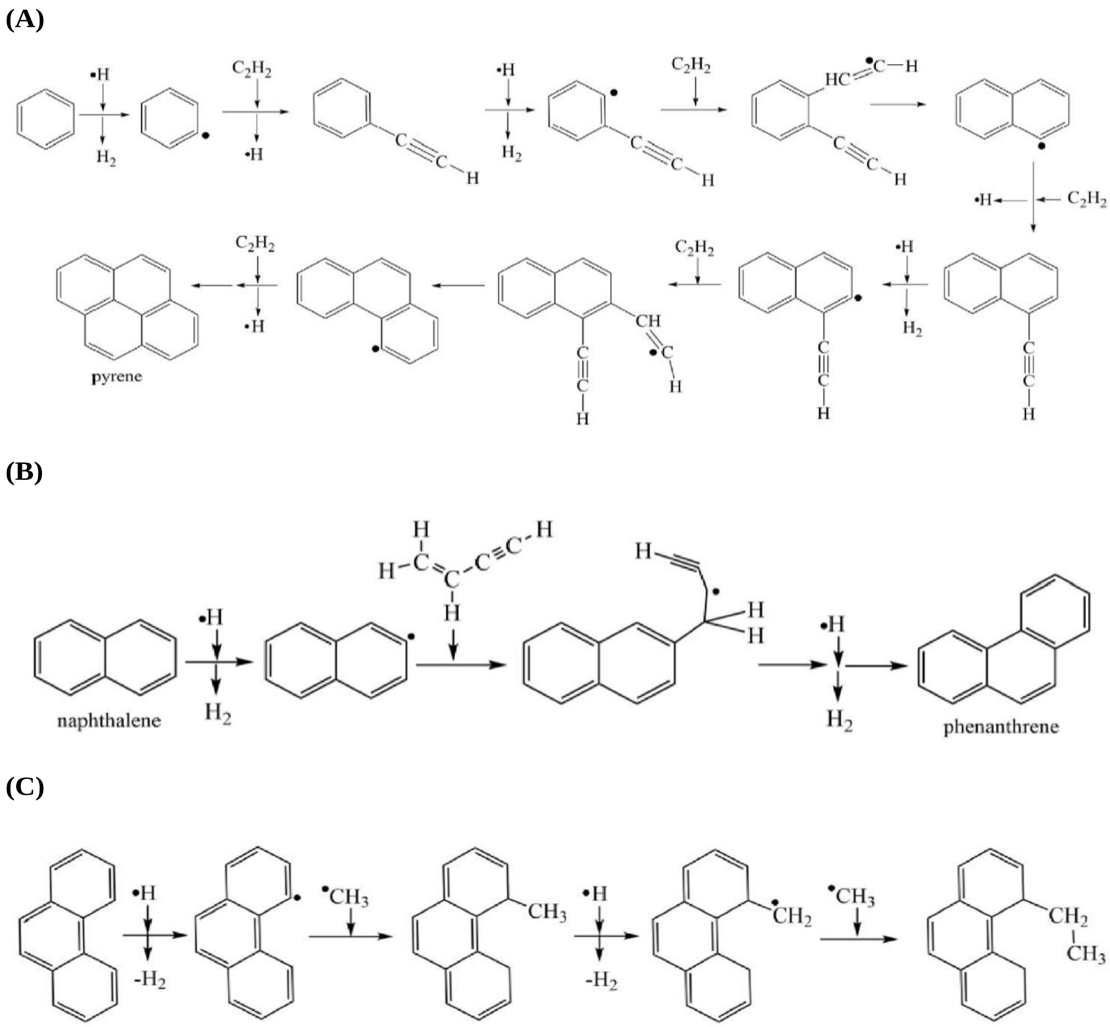

Figure 2.1 (A) the formation pathway of PYR via HACA mechanism, (B) the formation of PHE via HAVA mechanism, (C) The formation of an ethyl chain on PHE via the MAC mechanism (Reizer et al., 2022).

2.1.2 The toxicity of PAHs

The toxicity of the 16 PAHs has been frequently reported. For example, Sathikumaran et al. (2022) studied the toxicity symptoms of euryhaline fish named *Therapon Jarbua* exposed to B[α]P for 21 days with two distinct ambient concentrations. The authors examined the toxicity of different biomarkers such as deoxyribonucleic acid (DNA) damage in the gill and liver, serotonin, acetylcholinesterase, and ethoxyresorufin-

O-deethlylase. The results demonstrated that DNA damage and biotransformation enzyme levels increased with exposure time. Both the gill and the liver experienced dose-dependent ethoxyresorufin-O-deethlylase activation and DNA damage because of B[α]P exposure, albeit the liver's reaction was more linear. B[α]P poisoning increased the neurotoxicity by reducing acetylcholinesterase activity and serotonin levels in the brain. Tani et al. (2021) applied toxicity tests of many PAHs compounds on aquatic crustacean species such as *Daphnia magna* (48 h), and a benthic species, *Hyalella azteca* (96 h). Anthracene (ANT) and dibenz(a,h)anthracene were found to be non-toxic to both species after acute toxicity tests in the water exposure system, while half maximal effective concentration (EC_{50})/LC_{50} were determined as ranging from 0.66 (B[α]P) to 330 μg/L (PHE), and from 11 (1-aminopyrene) to 180 μg/L (PHE) for *D. magna* and *H. azteca*, respectively. In addition, Sun et al. (2020) investigated the adverse effect of benzo(a)anthracene (BaA) and fluoranthene (FLR) separately and mixed on the α-Amylase enzyme activity of the earthworm *Eisenia fetida* in soil. The findings demonstrated that BaA and FLR deeply impacted the microenvironment of α-Amylase's amino acid residue and its skeleton in separate and mixed pollutant systems. Furthermore, the mixed system had a greater inhibitory effect on α-Amylase activity than the separated one.

2.1.3 The sources of PAHs

According to the literature, the PAHs compounds could be released from two major sources:

(i) Natural sources such as forest fires, natural leakage, volcanic eruption, biological sources like diagenesis (organic transformation), and biogenic sources (plant, microbes, algae).

(ii) Anthropogenic sources (man-made) could be divided into two sources: Combustion sources (incomplete combustion of petroleum, gas, wood, etc).

Petrogenic sources are the products that are released from the processing and extraction of crude oil.

In general, the input of PAHs that come from natural sources is less than that from anthropogenic ones. Whatever the PAHs source, their mobility could be done through different pathways such as air deposition, river runoff, home and industrial emissions, direct spills of petroleum, etc (Wolska et al., 2012). In **Table 2.1**, several studies have been mentioned as a source of PAHs when they studied their concentration in different regions around the world in a different medium.

Table 2.1 The sources of PAHs that mentioned by some studies.

Main emission sources	Medium	Sample collection	Reference
1- Fuel oil 2- Wood burning and coal 3- Oil combustion	Chinese tea	purchased from the Chinese market	(Guo et al., 2022)
1- 54% from fossil fuel combustion 2- 29% from petrogenic inputs 3- 16% from vehicle exhaust emissions	Sediment	Chabahar Bay, Iran	(Seyed Hashtroudi et al., 2023)

Table 2.1 continued

Anthropogenic sources derived PAHs that are predominantly from pyrolytic origin	Surface sediments	Brunei Bay, Malaysia	(Sharifi et al., 2022)
The main PAH sources, 1- Motor vehicles 2- Heating in power plants and houses cooking 3- Combustion of wastes 4- Environmental tobacco smoke	Soil	Helsinki, Vilnius, Chicago, London, Tallinn	(Saltiene et al., 2002)
Direct petroleum combustion	Water	Lake Taihu, China	(Kong et al., 2021)
1- Historical contributions from multiple sources 2- A former coal gasification facility and petroleum product spills	Lake sediment	Owen Sound Bay Ontario, Canada	(Buell et al., 2021)

2.1.4 The detection and fates of PAHs in the environment

2.1.4 (a) The detection of PAHs Sediment

The presence of PAHs in sediments has been detected and assessed by different researchers. The distribution and the presence of the sediment vary from one place to another and that is extremely dependent on the physiochemical properties such as solubility, lipophilicity, and water vapor. PAHs molecules are detected in different places such as in river sediment, lake sediments, and marine sediments. For example, Tuncel & Topal (2015) collected sediment samples from 5 sites at Oludeniz Lagoon on the Turkish Mediterranean coast. They reported that PAHs were detected in 25 samples with a total concentration of 1.85 ± 1.39 mg/kg, acenaphthene and chrysene were the most dominant within the range of 0.620 and 0.515 mg/kg, respectively. The authors mentioned that the majority of the points are impacted by the burning of fossil fuels, followed by the burning of biomass and human activity. The PAHs were also detected in the river sediments, Chamorro et al. (2013) identified 45 organic microcontaminants in seven sediment samples from the Biobío River basin, including monoterpenes, sesquiterpenes, diterpenes, linear alkyl benzenes, PAHs, musk scents, sterols, and phthalate esters. The authors pointed out that the basin of Biobío River is influenced by domestic wastewater treatment, eucalyptus or pine Kraft pulp mills, and pyrolytic and pyrogenic processes. In addition, Andersson et al. (2014) identified the temporal characteristics and concentration variations of PAH during the last 5400 years in Lille Lungegårdsvannet lake sediments. The PAH data show relatively low concentrations before the industrial era, followed by a notable increase in their concentrations. It can be observed that the sources have changed with time, moving from pure wood and coal combustion in pre-industrial eras to mixed and petrogenic sources in more recent times.

2.1.4 (b) Detection of PAHs in soil

Pu et al. (2022) collected 27 samples of soil from four different basins of the Yangtze River located in Yichang in the western Hubei province, China. The PAHs concentrations were measured with the goal of determining their location, potential sources, and potential health concerns. The findings revealed that the surface soils contain PAHs within the range of 8.26 to 397 ng/g. They reported the average concentration of PAHs in valleys was 72.9 ng/g and 28.2 ng/g in the hilltop. They observed that PAHs with low molecular weight were dominant in both valleys and hilltops, and they suggested that the combustion of biomass and coal, followed by the burning of petroleum, is the primary source of PAHs on the soil surface. In addition, Shukla et al. (2022) gathered soil samples from the sides of the road in Lucknow, India, to examine the PAHs concentrations, origins, and potential cancer risks of 15 PAHs. The average concentration of 15 PAHs was determined to be 3748.23 ng/g, with a range between 478.94 to 8164.07 ng/g. Around 32.5% of the total samples were contained from four-ring PAHs, followed by six-ring 24.5% and around 16.7% five-ring PAHs. The researcher highlighted the dominance of petroleum, wood, coal, and grass combustion as sources of PAHs in the study area.

2.1.4 (c) Detection of PAHs in the atmosphere

Caliskan et al. (2020) collected ambient air samples were taken from two separate sites representing industrial and unregulated furniture manufacturing regions in order to measure the atmospheric PAHs concentrations in Inegol, Turkey. In the furniture workshops and industrial district districts, the mean ambient PAH concentrations measured in the gas phase were 697.82 ± 637 ng/m^3 and 772.92 ± 864.23 ng/m^3, respectively. In addition, in the furniture workshops site, the average total (gas + particle phases) concentration of 16 PAHs compounds was 1111.34 ± 1 045.24 ng/m^3, whereas, in the industrial district, it was 772.92 ± 864.23 ng/m^3. These values are higher than the reported ambient levels for urban locations with significant industries around the world. Additionally, due to local combustion sources, the average particle phase percentage was 30%. The principal component analysis results revealed that the major sources of pollution in the different regions are connected (combustion, traffic, industries). However, the uncontrolled burning of furniture waste as a fuel for home heating is regarded to be the most efficient source. Both regions' health risks for the population were calculated, and it was determined that they were not very high. PAHs were quantified using gas chromatography-mass spectrometry for samples collected throughout the Delhi-National Capital Region of India (Hazarika et al., 2019). The samples were collected to investigate the spatial and temporal variation of sixteen priority PAHs according to the classification of the USEPA. Throughout the investigations, it was shown that PAHs were strongly concentrated in the smaller size ranges of particles. In size-fractionated particles, B[α]P (12%) was the highest mean concentration, whereas acenaphthene (2%), contributed the least. In addition, around 7647 samples were collected during one year from 11 different urban sites in China by Ma et al. (2019) to measure 16 PAHs concentration. They revealed that the concentration of PAHs varied from site to site and PAHs' molar weight increased along with their proportional concentration in the particle phase. The average concentrations of 16 PAHs in northern and southern Chinese cities were 83.4 ± 151 ng/m^3 and 33.4 ± 45.5 ng/m^3, respectively.

2.1.4 (d) Detection of PAHs in the water

The current levels of PAHs in lake water settings are summarized by Meng et al. (2019). The findings showed that the quantities of PAHs in water ranged from 4.0 to 12,970.8 ng/L, and that naphthalene (NAP) (6525 ng/L) and indeno(1,2,3cd) pyrene (3452.6 ng/g) had the greatest amounts of each PAH. The Qinghai-Tibet Plateau Lakes District and the Mongolia-Xinjiang Lakes District were less polluted than other areas of the Great lakes' region in China. However, the pollution level of PAHs in lakes is relatively high on a global scale. The compositions and quantities of PAHs in Alexandria's coastal saltwater during the winter of 2015 are provided by El-Naggar et al. (2018). They revealed that the mean concentration value was found to be 991 ng/L within a range between 13.4 and 6076 ng/L, exceeding the maximum permissible amounts (200 ng/L) for the water standard of the European Union. The percentage distribution of the water samples revealed that around 41.7% of the examined samples had less than 500 ng/L, while 4.2% had greater than 6000 ng/L. The low molecular weight did not surpass 1.5%, and the four, five, and six rings made up 84%, 16.7%, and 5.5% of the total PAH, respectively. The authors mentioned that incomplete combustion of the fuel of boats and vehicle engines is the main source of PAHs, while pyrolytic origin occupied a small portion. Adeyeye et al. (2022) provided insight into the accumulative of PAHs in the sediments and fish parts on a fishpond. The studied PAHs were generally more concentrated in the sediments than in the water samples. The estimated coefficient of variation quantities showed that the PAHs level had a low (3.51-24.7%) geographic distribution. The fish included the highest concentrations of the chemicals FLR, PHE, and ANT.

2.1.4 (e) Detection of PAHs in the food, plants, and animals

One of the PAHs fates that have been mentioned is uptake by plants or detection in the food or in the animals' tissues and organs. For example, Alves et al. (2017) studied the presence of PHE, ANT, and PYR in the tissues of *Medicago sativa L*. (alfalfa) planted in soil artificially contaminated with 150 ppm of PAHs within 40 days. PAHs were detected in stomata, epidermal cells, injured areas, trichomes, and other places. Guo et al. (2022) calculate the concentration of PAHs concentration in the Chinese tea product, the authors revealed the 16 PAHs concentration ranged from 136.99 to 440.82 μg/kg and mainly contained from 2 and 4 rings. Furthermore, Qin et al. (2020) studied the tissue distribution and bioaccumulation of PAHs in freshwater organisms from Lake Chaohu, China. For carp, the brain had the highest level of PAHs, with a concentration of 591 ng/g. For bighead fish, the gills and muscles had the highest concentrations of PAHs 440 ng/g and 200 ng/g, respectively.

2.2 Soil remediation background

Soil, a vital element of terrestrial ecosystems, is a non-renewable resource. Unfortunately, it serves as a significant sink for various persistent pollutants that cannot be naturally degraded or eliminated (Sánchez-Castro et al., 2023). In this regard, it's become essential to develop a soil remediation system to avoid their direct, secondary, or tertiary adverse effects on human health and all over the ecosystem. The history of soil remediation can be traced back to the early 20th century, when soil contamination became a serious environmental issue due to rapid industrialization, urbanization, and agricultural intensification (Grifoni et al., 2022). **Figure 2.2** illustrates the evolution of soil remediation approaches from the 1970s until now. Idowu et al. (2019) reported that contaminated soil was categorized as hazardous waste, and the predominant disposal method was landfilling, largely driven by its lower implementation costs. This approach resulted from the misperception of contaminated soil as equivalent to general waste, leading to the application of waste treatment technologies in soil remediation. With time, soil remediation gained more attention and recognition as a scientific and engineering discipline, leading to the development of more advanced and innovative technologies based on physical, chemical, and biological agents (Lee et al., 2024). Recently, conventional soil remediation methods failed to consider the consequences of the remediation process, including aspects like the production of waste, the use of energy, societal acceptance, or the potential for both environmental sustainability and economic growth (Grifoni et al., 2022; Lamb et al., 2014; Lee et al., 2024).

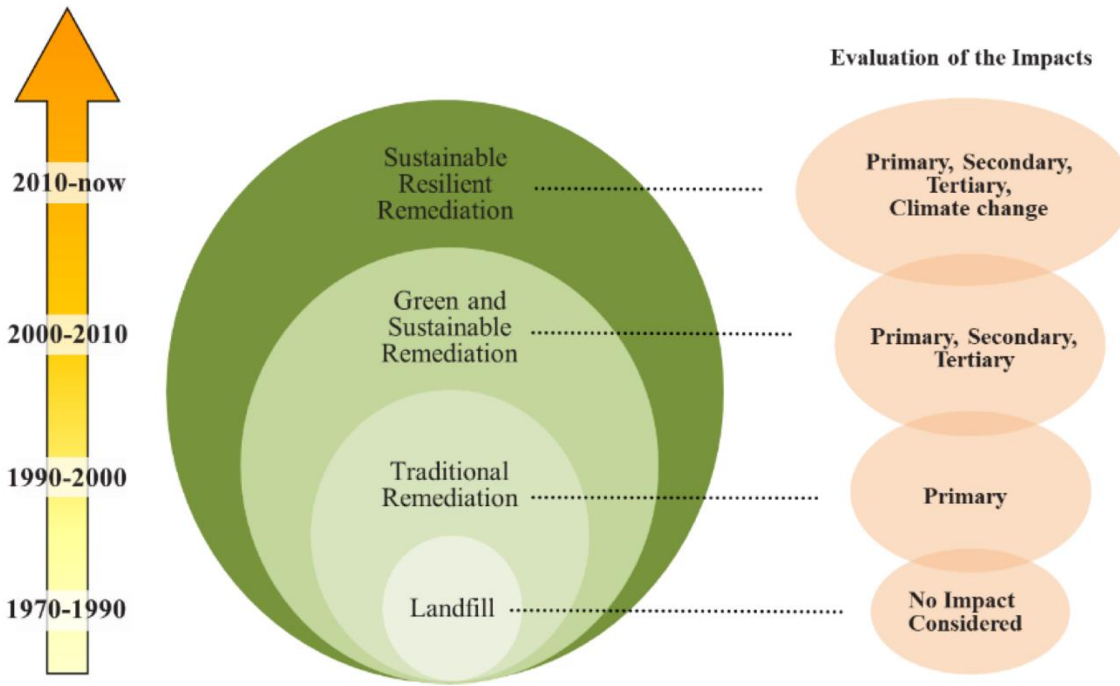

Figure 2.2 The evolution of soil remediation approaches (Grifoni et al., 2022)**.**

Based on the Scopus database, the search on the keyword "Soil remediation" showed that 39663 papers were published between 1984 and 2025 (Access date: 14 Feb 2024). In 1984, around 8 papers have been published. Year by year, the number of publications increased exponentially until reaching 3599 papers in 2023. This indicates that this field attracted more attention from environmentalists and soil pollution has become more challenging with the passing of time (**Figure 2.3**). Most of these publications were research articles and occupied 75% of the total publications, and conference papers, reviews, and book chapters occupied 10%, 8%, and 5%, respectively, while, the conference review, book, note, editorial, short survey, letter, retracted, erratum, abstract report, data paper, and report all of them occupied 2%.

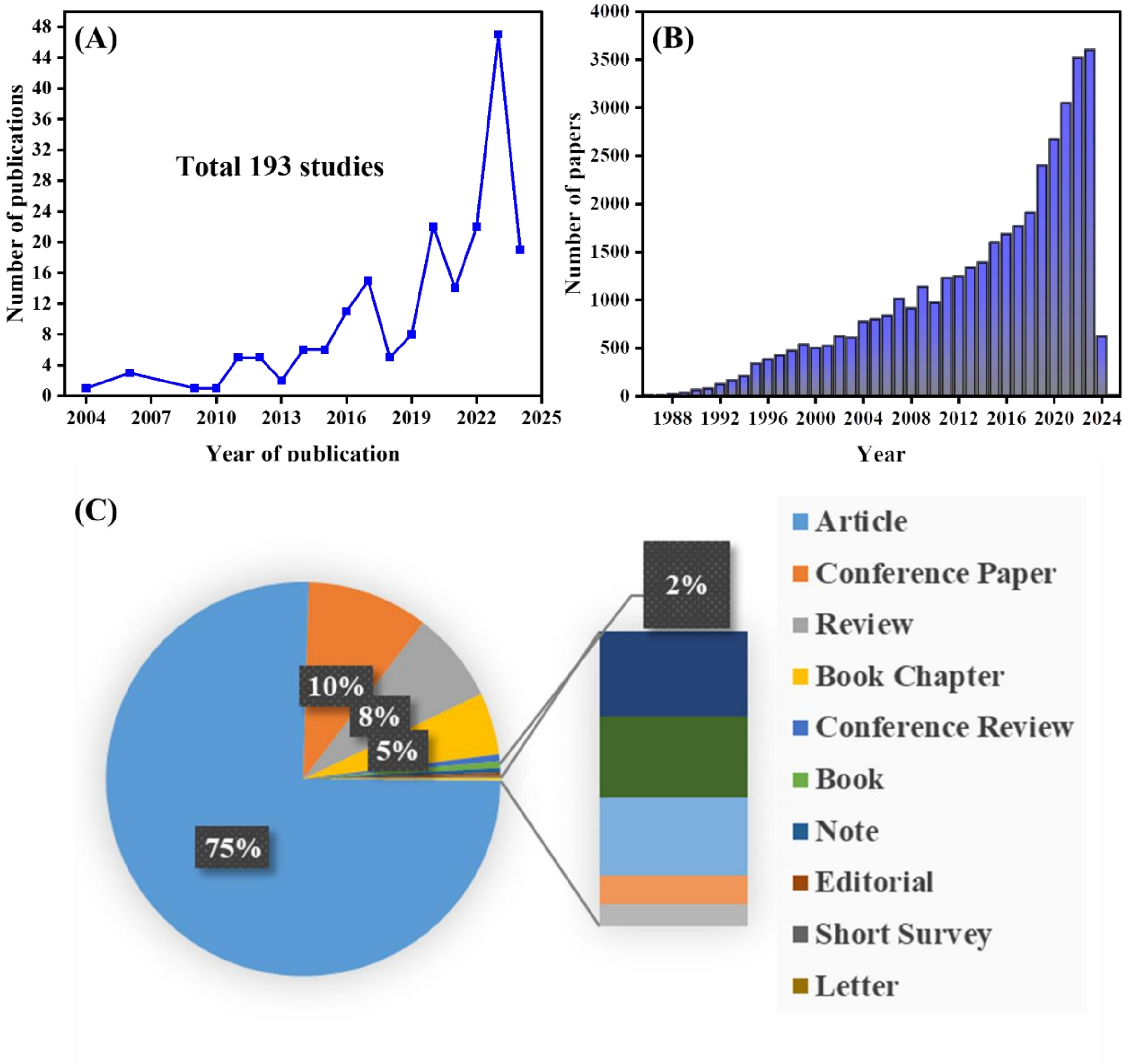

Figure 2.3 Bibliographic data since (A) the number of collected studies that are discussed in this chapter, (B) the number of published papers related to soil remediation, and (C) the type of publications.

2.3 Soil remediation from PAHs and other pollutants by various systems

Various methods have been employed to remediate tropical soils, tailored to address specific contaminants and soil conditions. Bioremediation leverages microbial activity to degrade organic pollutants, utilizing techniques such as natural attenuation, biostimulation, and bioaugmentation. Phytoremediation uses plants to absorb, stabilize, or degrade contaminants. Chemical oxidation, including AOPs with oxidants like hydrogen peroxide or persulfate, is often coupled with catalysts in tropical soils to enhance degradation efficiency. Soil washing, involving water or chemical solutions to extract pollutants. Thermal remediation applies heat to volatilize and remove organic contaminants, though it is less common in tropical regions due to high energy demands. Electrokinetic remediation uses electrical currents to mobilize contaminants toward electrodes for removal, effective for fine-grained soils but challenging in tropical settings due to soil conductivity. (Ashkanani et al., 2024; Tang et al., 2023).

2.3.1 Soil remediation via physicochemical techniques

2.3.1(a) Soil remediation based on electrokinetic techniques

Electrokinetic (EK) serves as an augmentative technique employed to address the limitations of bioremediation. It achieves this by elevating soil temperature and enhancing the bioavailability of nutrients. EK is notably effective, particularly in fine soil texture characterized by low hydraulic conductivity, distinguishing it from other in-situ methods. Zhu et al. (2024) discussed the use of an EK-citric acid system for remediating arsenic and cadmium-contaminated soil in karst areas. The results showed that 89.19% of oxidizable arsenic and 48.97% of acid-extractable arsenic are removed. Similarly, 60.88% of oxidizable cadmium and 87.87% of acid-extractable cadmium were removed.

Alkaline conditions promote the desorption and migration of arsenic in karst environments, while high calcium conditions inhibit the dissolution of arsenic but favor the dissolution of cadmium. Xu et al. (2021) performed a novel soil electrochemical remediation technology called flow-electrode capacitive deionization for the removal of heavy metals, specifically cadmium, from contaminated soil. The authors revealed that more than 80% of cadmium was removed from 200 g of kaolin under the optimum experimental conditions of carbon content of 50 g/L, a current density of 3.47 A/m^2, an initial pH of 3.2, and a sodium chloride concentration of 8.6 mmol/L. Santhosh et al. (2024) investigated the remediation of azodye-contaminated soil using EK and the evaluation of catalysts such as K_2SO_4 and NaCl for pollutant removal efficiency. The EK remediation process was conducted using a direct current of 10 V/cm for a duration of 56 h. The anode material used was ruthenium oxide (RuO_2), while the cathode material used was titanium oxide (TiO_2). The soil used in the experiment was contaminated with azodyes specifically methylene blue, trypan blue, congo red, and methylene red [Σ azo dyes] =100 mg/kg. The UV spectrum analysis showed that the concentration of the pollutant was higher in the cathode compared to the anode when using NaCl as the catalyst. Additionally, the chemical oxygen demand (COD) was achieved at a higher percentage (82%) in the NaCl catalyst compared to the K_2SO_4 catalyst, which achieved a COD removal rate of 62%. Bessaim et al. (2020) studied the role of process time in the removal of emerging salt contaminants from soil by EK technique. The experiments were conducted using two different treatment periods (3 and 5 days) and a voltage gradient of 1.5 V/cm. The results showed that increasing the treatment period enhanced the removal of monovalent cations and anions, including Na^+ and K^+, NO_3^-, and Cl^- with efficiency levels of 63%, 83%, 92%, and 63% respectively. Nevertheless, divalent cations and anions

(Ca^{2+}, Mg^{2+}, and SO_4^{2-}) showed irreversible behavior or less significant removal. Zhang et al. (2016) studied the effect of meteorological conditions on pollutant removal and enhancing approaches during photovoltaic energy direct application, using EK remediation of soil containing Cr(VI) as an example. The study revealed that meteorological conditions have a significant effect on pollutant removal efficiency, with the highest Cr(VI) removal efficiency (80.7%) observed within 60 min on a sunny day. Xu et al. (2020) introduced ion exchange membranes for the improvement EK process performed to remediate soil-containing PAHs. Ion-exchange membranes, particularly a cation-exchange membrane at the cathode, can enhance the EK in situ chemical oxidation process for the remediation of PAHs in contaminated soil. This system showed good removal efficiency and reached 93.1%. However, the authors reported that there was a significant change to the physical and chemical properties of the soil and consumed a substantial amount of power (2015 kWh/ ton). López-Vizcaíno et al. (2014) implemented EK remediation of natural soil polluted with PHE in a pilot plant. The results indicated that PHE is transported through the electroosmotic flow in the cathodic wells and by electrophoresis after the surfactant interacts with phenanthrene in the anodic wells. The authors mentioned that despite the long treatment time and high energy consumption, the average removal achieved was only 25%. Moreover, Zhou et al. (2016) combined EK remediation and modified activated alumina permeable reactive barrier for the treatment of fluorine-contaminated soil. They reported that this system can resolve the issue of fluorine accumulation in central and cathode regions that occurs with a single EK system. The removal efficiency of fluorine by combined remediation was 76% after 240 hours.

2.3.1(b) Soil remediation based on synthesized nanoparticles

Synthesized nanoparticles play a crucial role in the remediation of contaminated soil. These nanoparticles, due to their small size and high surface-to-volume ratio, can easily penetrate porous soil and reach pollutants. In the remediation, process they participate in adsorption and redox reactions, immobilizing and transforming contaminants into less harmful forms (Trivedi et al., 2022). A wide range of synthesized nanoparticles derived from different sources have been applied for soil remediation.

Among them, biochar (BC) attracted the researchers for several reasons. Firstly, BC is recognized for its non-toxic nature, affordability, and widespread availability. Secondly, its rich organic composition contributes significantly to enhancing soil fertility levels. Thirdly, BC's porous structure and expansive specific surface area enable efficient dispersion and stabilization of engineered nanoparticles, thereby augmenting their overall stability and mobility. Moreover, BC exhibits a substantial ion exchange capacity and hosts numerous oxygen-containing functional groups on its micropore surface, which are instrumental in reducing metal leaching and improving bioavailability in soil environments.

Su et al. (2016) developed a novel biochar-supported nanoscale zero-valent iron (nZVI@BC) for the in-situ remediation of Cr(VI)-contaminated soil. Through sedimentation tests and transport experiments, it was revealed that nZVI@BC with a nZVI to BC mass ratio of 1:1 exhibited superior stability and mobility compared to bare nZVI. Remarkably, when the soil was treated with 8 g/kg of nZVI@BC for 15 days, the immobilization efficiency of Cr(VI) and total chromium reached 100% and 92.9%, respectively. Wang et al. (2023) highlighted that employing a mass ratio of 1:4 between straw biochar and sludge resulted in a notable reduction in heavy metal content and effectiveness in soil. This approach also facilitated a shift in the morphology of copper (Cu) and lead (Pb) in heavy metal-contaminated soil, thereby achieving successful remediation of the contaminated soil. Li et al. (2024) coupling between magnetic BC and ryegrass to promote soil remediation from heavy metals. The results indicated a significant decrease in the concentrations of various heavy metals in soils, including Cr (24.12%), Ni (23.30%), Cu (22.01%), Zn (9.98%), As (14.83%), and Cd (15.08%). Ryegrass roots were identified as the primary accumulation site for heavy metals, with Zn showing the highest enrichment effect followed by As, Cr, Cu, Ni, and Cd. Wang et al. (2023) synthesized three types of BC derived from bamboo, coconut shell, and maize straw (MSB) for remediation of soil contaminated-PAHs and evaluation of an entire growth period of winter wheat. The utilization of three different types of biochar notably decreased the concentration of PAHs in the rhizosphere soil by 15.9%–33.7%. Regardless of the biochar type employed, it was observed that the degradation rate of high-molecular-weight PAHs exceeded that of low-molecular-weight PAHs. Additionally, all three varieties of biochar led to a significant increase in the relative abundance of dominant bacterial phyla and genera in the soil. **Table 2.2** presents studies investigating soil remediation using different synthesized particles including biochar.

Table 2.2 Studies investigated soil remediation using different synthesized particles.

Synthesized particles	Target pollutant	Experimental conditions	Removal	Process time	References
$MgFe_2O_4$/chitosan carbon aerogel beads	Cadmium	3 g carbon aerogel beads were fully mixed with 100 g cadmium-contaminated.	72.27%	14 days	(Li et al., 2024)